HHS Public Access

Author manuscript

Nat Chem. Author manuscript; available in PMC 2010 March 13.

Published in final edited form as:

Nat Chem. 2009 September 13; 1: 562–567. doi:10.1038/nchem.360.

An Optoelectronic Nose for Detection of Toxic Gases

Sung H. Lim[§,†], **Liang Feng**[‡,†], **Jonathan W. Kemling**[‡], **Christopher J. Musto**[‡], and **Kenneth S. Suslick**[‡,*]

[‡] Department of Chemistry, University of Illinois at Urbana-Champaign, 600 S. Mathews Ave., Urbana, Illinois 61801 USA

[§] iSense LLC, 470 Ramona St., Palo Alto, CA 94301 USA

Abstract

We have developed a simple colorimetric sensor array (CSA) for the detection of a wide range of volatile analytes and applied it to the detection of toxic gases. The sensor consists of a disposable array of cross-responsive nanoporous pigments whose colors are changed by diverse chemical interactions with analytes. Although no single chemically responsive pigment is specific for any one analyte, the pattern of color change for the array is a unique molecular fingerprint. Clear differentiation among 19 different toxic industrial chemicals (TICs) within two minutes of exposure at IDLH (immediately dangerous to life or health) concentration has been demonstrated. Quantification of each analyte is easily accomplished based on the color change of the array, and excellent detection limits have been demonstrated, generally below the PELs (permissible exposure limits). Identification of the TICs was readily achieved using a standard chemometric approach, i.e., hierarchical clustering analysis (HCA), with no misclassifications over 140 trials.

There is an obvious pressing need for rapid, sensitive and highly portable identification of toxic gases and vapors, not only from a security perspective, but also for use in the industrial chemical workplace and for more general epidemiological studies1. Almost by definition, toxic industrial chemicals (TICs) are chemically reactive. Their toxicities, however, derive from a very wide range of specific chemical reactivities that can affect vastly different systems within living organisms. Some acute toxins target specific, critical metabolic enzymes (e.g., HCN inhibits cytochrome c oxidase), others cause cell lysis in the lungs

*Corresponding author: (tel) 1-217-333-2794; (fax) 1-217-333-2685; ksuslick@illinois.edu.
†Contributed equally to this work

Author contributions

S.H.L. and L.F. contributed equally to the design of experiments, collection and analysis of data, and drafting of the manuscript with assistance from J.W.K. and C.J.M. K.S.S. originated the central idea, oversaw design of experiments and data analysis, and contributing to the writing of the manuscript.

Additional information

Supplementary Information accompanies this paper at www.nature.com/naturechemistry. Reprints and permission information is available online at www.npg.nature.com/reprintsandpermissions/. Correspondence and requests for materials should be addressed to K.S.S.

Competing financial interests

K.S.S. discloses his status as a major shareholder of ChemSensing, whose software was used in image analysis in this work, and in iSense LLC, employer of one of the co-authors (S.H.L).

creating pulmonary edema (e.g., HCl, HF). Others are potent oxidants or reductants that can target multiple biosystems, and some are potent alkylating agents (e.g., phosgene). We approach the detection and identification of TICs by presenting a wide range of chemical substrates whose reactions with these analytes provide an easily observable response, specifically color changes quantified by digital imaging. Such an “optoelectronic nose” is an array-based chemical sensing founded on the biomimetic concept of using many cross-responsive sensor elements2–5, rather than analyte-specific lock-and-key receptors. As with the mammalian olfactory system7–9, it is the composite response of the chemical reactivity of such an array that identifies an odorant or mixture of odorants. Our optoelectronic nose uses a colorimetric sensor array that largely overcomes the limitations of prior electronic nose technologies, and we report here its use for the identification of a wide range of TICs at low concentrations.

In contrast to our chemical reactivity approach, prior electronic nose technology10–19 generally relies on sensors whose responses originate from weak and highly non-specific chemical interactions that either induce changes in physical properties (e.g., mass, volume, conductivity) or follow after physisorption on surfaces (i.e., analyte oxidation on heated metal oxides). Specific examples of such sensors include conductive polymers and polymer composites, multiple polymers doped with single fluorescent dye, polymer coated surface acoustic wave (SAW) devices, and metal oxide sensors. As a consequence of this reliance on weak interactions, most prior electronic nose technology suffers from severe limitations: the detection of compounds at low concentrations relative to their vapor pressures is difficult; the discrimination between compounds within a similar chemical class is limited; and importantly, interference from environmental changes in humidity remains problematic.

The design of our colorimetric sensor array2–5, 20–27 (CSA) is based on stronger dye-analyte interactions than those that cause simple physical adsorption; the array incorporates a chemically diverse set of chemically responsive colorants, including metalloporphyrins and chemically responsive dyes. More specifically, we have chosen chemically responsive dyes in four classes (cf. Fig. 1): (1) metal ion containing dyes (e.g., metalloporphyrins) that respond to Lewis basicity (i.e., electron pair donation, metal ion ligation), (2) pH indicators that respond to Brønsted acidity/basicity (i.e., proton acidity and hydrogen bonding), (3) dyes with large permanent dipoles (e.g., vapochromic or solvatochromic dyes) that respond to local polarity, and (4) metal salts that respond to redox reactions. The importance of including metal ion containing sensors in such an array is confirmed by the indications that the mammalian olfactory receptors are likely metalloproteins8–9. In recent related work, we have reported25–27 a new array methodology specifically for liquid sensing that is based on nanoporous pigments created by the immobilization of pH indicators in organically modified siloxanes (ormosils)28. Nanoporous pigments offer substantial advantages over soluble dyes for improved durability and stability of the array, as well as prevention of colorant leaching in aqueous media. Here, we report an extension of these new nanoporous pigment arrays using a much broader range of chemically responsive pigments, apply the arrays for the colorimetric identification of TICs in the gas phase, and demonstrate substantial improvements in the array sensitivity at low gas concentrations.

Results and Discussion

The chemically responsive indicators used in prior colorimetric sensor arrays have been limited to soluble molecular dyes held in a semi-fluid polymer film and generally printed onto a porous membrane2–5, 20–24. Relative to insoluble pigments, chemically responsive dyes in semi-fluid state are often unstable over long periods of storage. Non-porous pigments, on the other hand, generally do not provide sufficient contact between the analyte and the chromophores of the pigment, because the chromophores at the surface of the pigment are generally only a small fraction of the total number of chromophores.

There is, however, a general method to the incorporation of chemically responsive dyes into porous matrices, thus creating nanoporous pigments that can provide both stability and analyte access to the chromophores. Among various host materials, ormosils provide excellent matrices for a variety of organic and inorganic colorants28–31. Furthermore, the final properties of the nanoporous pigments (e.g., hydrophobicity, porosity, and surface area) can be easily modified by controlling the physical and chemical parameters of the sol-gel process. For our printing of sensor arrays, we prepared sol-gel-colorant solutions by the simple hydrolysis of solutions containing commercially available silane precursors (e.g., tetraethoxysilane, methyltriethoxysilane, phenethyltrimethoxysilane and octyltriethoxysilane) with a variety of chemically responsive indicators.

This conversion of soluble dyes into nanoporous ormosil pigments significantly improves stability28–31: we find that there is no change in the analyte response for arrays stored for more than three months27. Importantly, our sol-gel formulation permits the simple printing onto ordinary polymer flat surfaces, which has allowed us an easy packaging of the sensor array into a self-sealing cartridge with minimal dead-space (Supplementary Fig. S1) suitable for use with a handheld battery-operated scanner (Supplementary Fig. S2). In addition, we find that the porous matrix improves the sensitivity of the sensor; compared to prior results with highly plasticized dye sensor arrays, we find an improvement in sensitivity of ~800% at low concentrations. We hypothesize that the nanoporous matrix may serve as an *in situ* preconcentrator for analytes.

As an important application of this new optoelectronic nose, we have begun an examination of TICs, choosing 19 representative examples from lists generated by the International Task Force 25 and 40 reports32–33. The IDLH concentrations of these TICs are given in Supplementary Table S2. Detection and discrimination among the wide range of high priority TICs remains a major challenge34 and the subject of substantial recent research. For example, Hammond et al. recently reported35 on TIC identification using an array of ceramic metallic films; they were able to different-tiate among ten TICs with an error rate of ~10% using a linear discriminant analysis. Using metal oxide detectors combined with temperature programming, Meier et al. examined36 five toxic industrial chemicals and were able to reduce their error rate (both false negatives and positives) to 3%.

We have extensively tested our colorimetric sensor array against 19 TICs at their IDLH concentrations at 50% relative humidity (RH). The colorimetric sensor arrays were exposed for two minutes to a diluted gas mixture produced either from pre-mixed, certified gas

cylinders or from saturated vapor, using digital mass flow controllers (configurations shown in Supplementary Fig. S3). Importantly, gas stream concentrations were confirmed by in-line analysis by FT-IR in real time using a MKS multi-gas analyzer for most analytes or by Dräger detector tubes in the few cases where FT-IR cannot be used (e.g., homonuclear diatomics Cl_2 and F_2).

The printed arrays were digitally imaged with an ordinary flatbed scanner before and after exposure to each analyte. Color difference maps for the arrays were generated by subtraction of the image before exposure from the image after exposure: such a difference map provides a molecular fingerprint that effectively identifies the analyte to which the array has been exposed. The difference maps permit facile detection and identification of the 19 representative TICs, as shown in Fig. 2. Even by eye, without statistical analysis, the array response to each TIC is represented by a unique pattern. For quantitative analysis of the difference maps, we can define a 108-dimensional vector (i.e., 36 changes in red, green and blue values for the after exposure image compared to the before exposure image for our 6×6 array of nanoporous pigments). In this fashion, it is not necessary to retain the full digital images: each analyte is represented digitally by the 108-dim. vector and may be compared by standard chemometric techniques. Simple comparisons of the Euclidean distance between an observed color difference vector and a pre-collected library are extremely rapid (sub-second); even a large library requires only minimal memory (e.g., 1000 entries needs 148 KB zip compressed). The raw digital color difference vectors from a total of 140 experimental trials are given in Supplementary Tables S3 and S4.

For most analytes, the response of these colorimetric sensor arrays is based primarily on equilibrium interactions between the array pigments and the analyte, and consequently, each concentration of a TIC has a separate pattern which can be used to establish a limit of detection. As examples, color change profiles for three different analytes as a function of concentration can be seen in Fig. 3. Here the limits of detection (LODs) for all three examples are well below their respective PELs. While highly dependent on the analyte, our estimates for the LOD for TICs examined here are all well below their respective PELs.

Most of the TICs can be identified from the array color change in a matter of seconds, and >90% of total response is observed in less than two minutes, as shown in Fig. 4 for five representative TICs; all other TICs tested show very similar responses. For some aggressive analytes that undergo irreversible reactions with some pigments (e.g., bleaching), response time can be slightly longer, as demonstrated for Cl_2 (Fig. 4), but even in these cases the color change pattern is distinctive and easily recognized.

While the CSAs are meant to be disposable, they are still re-usable for most analytes. The CSA is best thought of as a “chemical fuse”: just as with an electric fuse, as long as the concentration of the odorant (i.e., “the electric current”) fluctuates within some range, the CSA (“fuse”) is unaffected. But, if the concentration increases to too high a value, the CSA will take too long to recover: i.e., the fuse is blown and the CSA should be replaced. As illustrated in Fig. 5a, the CSA will reproducibly cycle between the IDLH and PEL concentrations of many toxic industrial chemicals (SO_2 as an example). After switching from one concentration to the other, equilibrium response is achieved within two minutes.

The reversibility of the array is dependent on the type of chemical interaction between the pigments and the analytes, and for irreversible reactions with highly aggressive analytes (e.g., those capable of bleaching or redox reactions), the array cannot be recycled as demonstrated in Fig. 5b for Cl_2. For other gases, notably arsine and phosphine, it is the reduction of metal salts generating metal nanoparticles that produces acidic byproducts that are detected by pH indicators incorporated into the nanoporous sol-gel spot. Finally, the response to phosgene is due to an alkylation reaction with 4-(4-nitrobenzyl)pyridine within the sol-gel matrix.

In real world situations, one is unlikely to have control over the humidity, which can be extremely problematic for prior electronic nose technologies. Because both our colorants and the sol-gel matrices are selected to be hydrophobic, we find that changes in humidity present no difficulty. As shown in Supplementary Fig. S4, the color difference maps are unaffected by changes in RH from 10% to 90%.

The color change profiles are inherently digital data and are easily handled by routine chemometric analysis37–40. The high dispersion of the colorimetric sensor array data requires a classification algorithm that uses the full dimensionality of the data. The simplest statistical approach is hierarchical cluster analysis (HCA), which is a classification scheme based on the Euclidean distance between data points in their full dimensionality. The advantage of HCA compared to other model-dependent statistical analysis (e.g. linear discriminant analysis) is that it makes no assumptions about the classification of results that one is trying to establish. Each experimental trial is defined as a 108-dimensional vector consisting of the changes in red, green, and blue values of each of the 36 nanoporous pigments in our array. Hierarchical clustering is based on the Euclidean distance in this 108-dimensional ΔRGB color space among these vectors, which generates a dedrogram, as shown in Figure 6. Remarkably, in septuplicate trials, all 19 TICs and a control were accurately identified against one another *with no errors or misclassifications out of 140 cases.*

The ability of our CSAs to discriminate so many analytes from one another is impressive and is due largely to the extremely high dimensionality of the array data. Principal component analysis (PCA) can be used to determine the number of meaningful independent dimensions probed by a cross-reactive array. The eigenvector of each principal component defines the linear combination of the response of each sensor parameter by the amount of variance in the data along each principal component. Based on the 140 trials on 20 analytes (i.e., 19 TICs plus background), the PCA of our colorimetric sensor array requires 9 dimensions for 90% of total variance (and 13 dimensions for 95%, as shown in Supplementary Fig. S5). This extremely high dispersion reflects the very wide range of chemical-properties space being probed by our choice of chemoresponsive pigments. As a consequence, chemically diverse analytes are easily recognizable and even closely related mixtures can be distinguished2–4. In contrast, data from most prior electronic nose technology are dominated by only two or three independent dimensions (one of which, analyte hydrophobicity, generally accounts for >90% of total variance); this is the inherent result of relying on van der Waals and other weak interactions (e.g., adsorption to metal oxide surfaces or absorption onto or into polymer films) for molecular recognition.

Conclusions

In summary, we have created a simple, disposable colorimetric sensor array of nanoporous pigments that is capable of detecting a wide range of analytes. By immobilizing chemically responsive indicators within nanoporous sol-gel matrices, we can apply the sensor array to the detection of volatile toxic industrial chemicals and observe low detection limits, generally below the permissible exposure levels. Classification analysis reveals that the colorimetric sensor array has an extremely high dimensionality and consequently the ability to discriminate among large numbers of TICs over a wide range of concentrations.

While the laboratory studies reported here made use of inexpensive flatbed scanners for imaging, we have recently constructed a fully functional prototype handheld device that makes use of inexpensive white LED illumination and an ordinary CMOS camera, as shown in Supplementary Fig. S2; indeed, the signal-to-noise of the images taken with this prototype are a factor of 3 better than our flatbed scanners. Combined with a low dead volume cartridge (Supplementary Fig. S1), this handheld presents a rapid, inexpensive, and highly sensitive method for portable monitoring of ambient toxic gases. Further development, we expect, will lead to a wearable device: i.e., the chemist's equivalent of a physicist's radiation badge.

Methods

Reagents

All reagents used were analytical-reagent grade and obtained from Sigma-Aldrich and used without any further purification unless otherwise specified. Certified, premixed gas tanks, including ammonia, methylamine, dimethylamine, trimethylamine, HCl, SO_2, fluorine, chlorine, phosphine, arsine, phosgene, hydrogen sulfide, hydrogen cyanide, and diborane were obtained from Matheson Tri-Gas Corp. through S. J. Smith, Co. (Urbana, IL).

Array Printing

The colorant indicators are given in Supplementary Table S1. Final organically modified sol-gel (ormosil) formulations with the colorants were loaded into a 36-hole Teflon ink well. Sensor arrays were printed using an array of 36 floating slotted pins (which delivered approximately 130 nL each) by dipping into the ink well and transferring to the PET film. Once printed, the arrays were aged under nitrogen for at least 3 days before any sensing experiment was performed.

Experimental Procedure

The toxic industrial chemicals at their IDLH concentrations (cf. Supplementary Table S2) were prepared by mixing the prediluted analyte gas stream with dry and wet nitrogen gas with MKS digital mass flow controllers to achieve the desired concentrations and relative humidity (RH) (cf. Supplementary Fig. S2). For nitric acid and HF, saturated vapors were generated from a diluted solution in a five gallon polyethylene carboy, which was further diluted to IDLH concentration with nitrogen gas. Hydrazine (98%) was used directly to produce saturated hydrazine vapor. Importantly, gas stream concentrations and relative

humidity were confirmed by in-line analysis by FTIR using a MKS multi-gas analyzer, model 2030. In our experience, *independent in-line analysis of tank gases is absolutely essential*, even with the manufacturer's certification; premixed tanks of these reactive gases at the low concentrations used here (typically four times the IDLH) do not necessarily retain their original certified concentrations. Fluorine, chlorine, hydrazine, nitric acid and HF at their IDLH concentrations were confirmed using Dräger detector tubes.

Data Analysis

For all sensing experiments, imaging of the arrays was done on an ordinary flatbed scanner (Epson Perfection V200); for good reproducibility, it is important to "warm-up" the scanner. Difference maps were obtained by taking the difference of the red, green, and blue (RGB) values from the center of every colorant spot (~300 pixels) from the "before" and "after" images. To eliminate the possibility of subtraction artifacts caused by variations in color near the spot edge, only the spot center is included in the calculation. Averaging of the centers of the spots avoids artifacts from non-uniformity of the printing of the spots, especially at their edges. Subtraction of the two images yields a color difference vector of 3N dimensions where N=total number of spots; for our six by six array, this difference vector is 108 dimensions (i.e., 36 changes in red, green, and blue color values), each dimension ranging from −255 to +255 for 8-bit color imaging). The difference vectors are provided in Supplementary Tables S3 and S4. Measurements can be performed using Adobe Photoshop™or with a customized software package, ChemEye™ (ChemSensing, Inc., Champaign, IL). All experiments were run in septuplicate, and chemometric analysis was carried out on the difference vectors using the Multi-Variate Statistical Package™ (v. 3.1, Kovach Computing).

Humidity experiments

Relative humidity was controlled by mixing dry N_2 with humidity saturated N_2 (100% RH, generated from bubbling N_2 through water). Using 50% RH as a control, arrays were exposed to various humidity concentrations for two minutes. (cf. Supplementary Fig. S4); no significant response to humidity was observed from 10 to 90% RH.

Cycling Experiments

SO_2 and chlorine gases at PEL concentrations were prepared using the same method as IDLH concentration. The colorimetric sensor array was exposed to N_2 (50% RH) for 5 minutes, and then the gas stream switched from IDLH to PEL and back every 10 minutes. Data was acquired every minute.

Supplementary Material

Refer to Web version on PubMed Central for supplementary material.

Acknowledgments

This work was supported through the NIH Genes, Environment and Health Initiative through award U01ES016011.

References

1. Byrnes, ME.; King, DA.; Tierno, PM, Jr. Nuclear, Chemical, and Biological Terrorism—Emergency Response and Public Protection. CRC Press; Boca Raton, FL: 2003.
2. Suslick KS, et al. Seeing smells: development of an optoelectronic nose. Quimica Nova. 2007; 30:677–681.
3. Suslick KS. An optoelectronic nose: seeing smells by means of colorimetric sensor arrays. MRS Bulletin. 2004; 29:720–725. [PubMed: 15991401]
4. Suslick KS, Rakow NA, Sen A. Colorimetric sensor arrays for molecular recognition. Tetrahedron. 2004; 60:11133–11138.
5. Rakow NA, Suslick KS. A colorimetric sensor array for odour visualization. Nature. 2000; 406:710–713. [PubMed: 10963592]
7. Hawkes, CH.; Doty, RL. The Neurology of Olfaction. Cambridge University Press; Cambridge: 2009.
8. Zarzo M. The sense of smell: molecular basis of odorant recognition. Biol Rev. 2007; 82:455–479. [PubMed: 17624963]
9. Wang J, Luthey-Schulten ZA, Suslick KS. Is the olfactory receptor a metalloprotein? Proc Natl Acad Sci USA. 2003; 100:3035–3039. [PubMed: 12610211]
10. Gardner, JW.; Bartlett, PN. Electronic Noses: Principles and Applications. Oxford University Press; New York: 1999.
11. Lewis NS. Comparisons between mammalian and artificial olfaction based on arrays of carbon black-polymer composite vapor detectors. Acc Chem Res. 2004; 37:663–672. [PubMed: 15379582]
12. Röck F, Barsan N, Weimar U. Electronic nose: current status and future trends. Chem Rev. 2008; 108:705–725. [PubMed: 18205411]
13. Hierlemann A, Gutierrez-Osuna R. Higher-order chemical sensing. Chem Rev. 2008; 108:563–613. [PubMed: 18198903]
14. Anslyn EV. Supramolecular analytical chemistry. J Org Chem. 2007; 72:687–699. [PubMed: 17253783]
15. Walt DR. Electronic noses: wake up and smell the coffee. Anal Chem. 2005; 77:45 A.
16. Wolfbeis OS. Materials for fluorescence-based optical chemical sensors. J Mater Chem. 2005; 15:2657–2669.
17. Hsieh MD, Zellers ET. Limits of recognition for simple vapor mixtures determined with a microsensor array. Anal Chem. 2004; 76:1885–1895. [PubMed: 15053648]
18. Janata J, Josowicz M. Conducting polymers in electronic chemical sensors. Nat Mater. 2003; 2:19–24. [PubMed: 12652667]
19. Grate JW. Acoustic wave microsensor arrays for vapor sensing. Chem Rev. 2000; 100:2627–2647. [PubMed: 11749298]
20. Rakow NA, Sen A, Janzen MC, Ponder JB, Suslick KS. Molecular recognition and discrimination of amines with a colorimetric array. Angew Chem Int Ed. 2005; 44:4528–4532.
21. Janzen MC, Ponder JB, Bailey DP, Ingison CK, Suslick KS. Colorimetric sensor arrays for volatile organic compounds. Anal Chem. 2006; 78:3591–3600. [PubMed: 16737212]
22. Zhang C, Suslick KS. A colorimetric sensor array for organics in water. J Am Chem Soc. 2005; 127:11548–11549. [PubMed: 16104700]
23. Zhang C, Bailey DP, Suslick KS. Colorimetric sensor arrays for the analysis of beers: a feasibility study. J Agric Food Chem. 2006; 54:4925–4931. [PubMed: 16819897]
24. Zhang C, Suslick KS. Colorimetric sensor array for soft drink analysis. J Agric Food Chem. 2007; 55:237–242. [PubMed: 17227048]
25. Lim SH, Musto CJ, Park E, Zhong W, Suslick KS. A colorimetric sensor array for detection and identification of sugars. Org Lett. 2008; 10:4405–4408. [PubMed: 18783231]
26. Bang JH, Lim SH, Park E, Suslick KS. Chemically responsive nanoporous pigments: colorimetric sensor arrays and the identification of alipathic amines. Langmuir. 2008; 24:13168–13172. [PubMed: 18950204]

27. Musto CJ, Lim SH, Suslick KS. Colorimetric detection and identification of natural and artificial sweeteners. Anal Chem. in press.
28. Podbielsk, H.; Ulatowska-Jarza, A.; Muller, G.; Eichler, HJ. Optical Chemical Sensors. Springer; Erice, Italy: 2006.
29. Dunbar RA, Jordan JD, Bright FV. Development of chemical sensing platforms based on sol-gel-derived thin films: origin of film age vs. performance trade-offs. Anal Chem. 1996; 68:604–610.
30. Jeronimo PCA, Araujo AN, Montenegro M. Optical sensors and biosensors based on sol-gel films. Talanta. 2007; 72:13–27. [PubMed: 19071577]
31. Rottman C, Grader G, De Hazan Y, Melchior S, Avnir D. Surfactant-induced modification of dopants reactivity in sol-gel matrixes. J Am Chem Soc. 1999; 121:8533–8543.
32. Steumpfle, AK.; Howells, DJ.; Armour, SJ.; Boulet, CA. Final Report Of International Task Force-25: Hazard From Toxic Industrial Chemicals. US GPO: Washington, DC; 1996. http://file.sunshinepress.org:54445/us-uk-ca-mou-itf25-1996.pdf
33. Armour SJ, et al. International Task Force 40: Toxic Industrial Chemicals (TICs -Operational and Medical Concerns. http://chppm-www.apgea.army.mil/desp/pages/jeswg/4QFY01/itf-40-2US.ppt
34. Hill HH, Martin SJ. Conventional analytical methods for chemical warfare agents. Pure Appl Chem. 2002; 74:2281–2291.
35. Hammond MH, et al. A novel chemical detector using cermet sensors and pattern recognition methods for toxic industrial chemicals. Sens Actuators, B. 2006; B116:135–144.
36. Meier DC, et al. The potential for and challenges of detecting chemical hazards with temperature-programmed microsensors. Sens Actuators, B. 2007; B121:282–294.
37. Hasswell, S. Practical Guide To Chemometrics. Dekker; New York: 1992.
38. Scott SM, James D, Ali Z. Data analysis for electronic nose systems. Microchim Acta. 2007; 156:183–207.
39. Johnson, RA.; Wichern, DW. Applied Multivariate Statistical Analysis. 6. Prentice Hall; Upper Saddle River, NJ: 2007.
40. Hair, JF.; Black, B.; Babin, B.; Anderson, RE.; Tatham, RL. Multivariate Data Analysis. 6. Prentice Hall; Upper Saddle River, NJ: 2005.

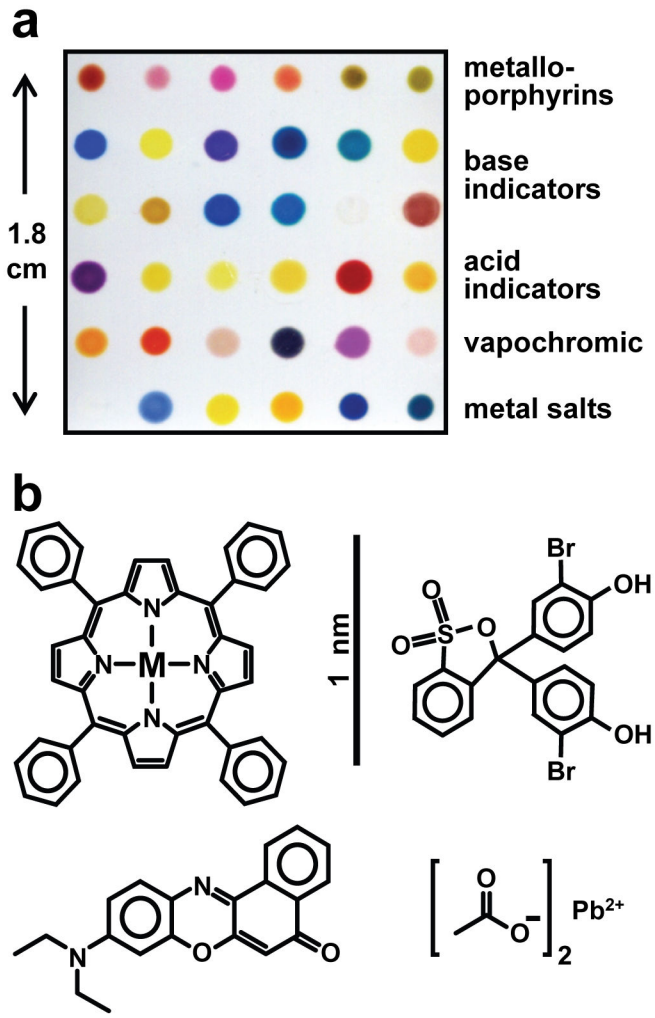

Fig. 1. The colorimetric sensor array (CSA) consists of 36 different chemically responsive pigments that have been printed directly on a polyethylene terephthalate (PET) film

a An image of the array from an ordinary flatbed scanner with the different pigment classes labeled. **b.** Molecular structures of examples from each dye class are shown; in order to absorb visible light, dyes are inherently nanoscale, as noted by the scale bar. The 36 dyes were selected empirically based on the quality of their color response to a representative selection of chemically diverse analytes.

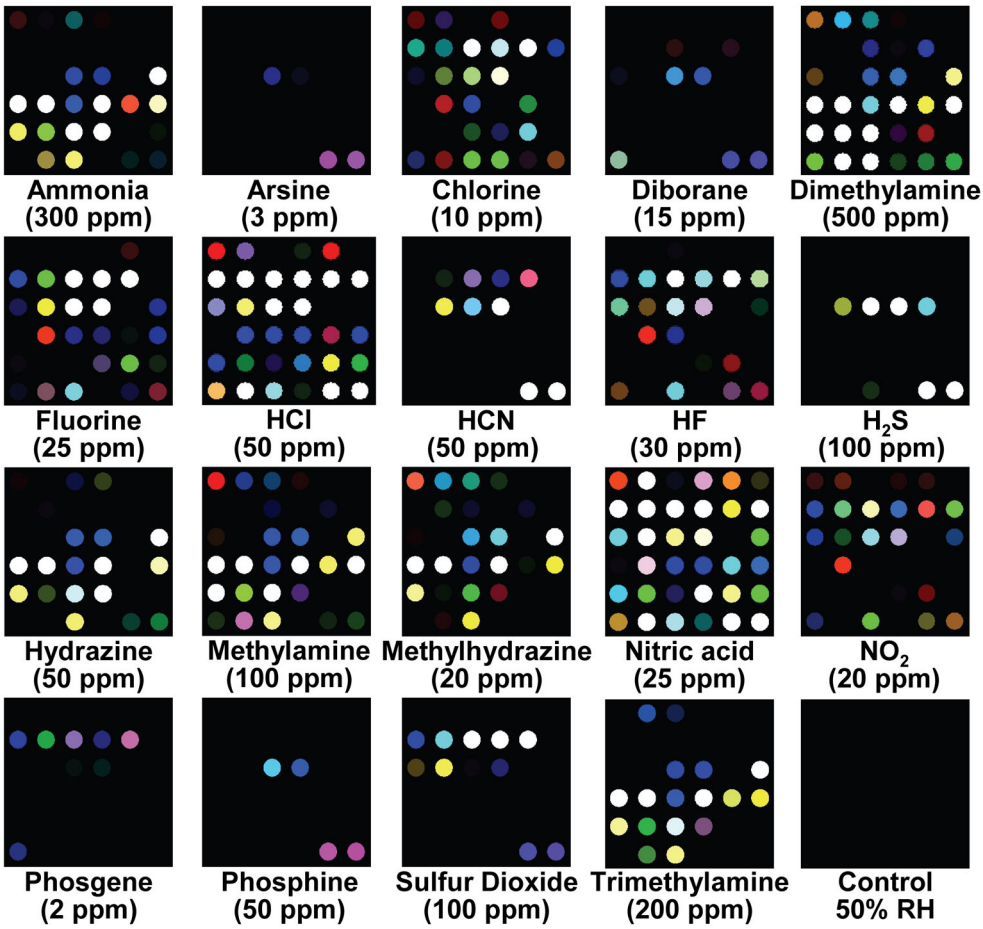

Fig. 2. Color change profiles of representative toxic industrial chemicals (TICs) at their IDLH (immediately dangerous to life or health) concentration after 2 min of exposure

The IDLH concentrations are listed under each analyte in ppm. A full digital database is provided in the Supplementary Table S3. For display purposes, the color range of these difference maps are expanded from 4 to 8 bits per color (RGB range of 4–19 expanded to 0–255).

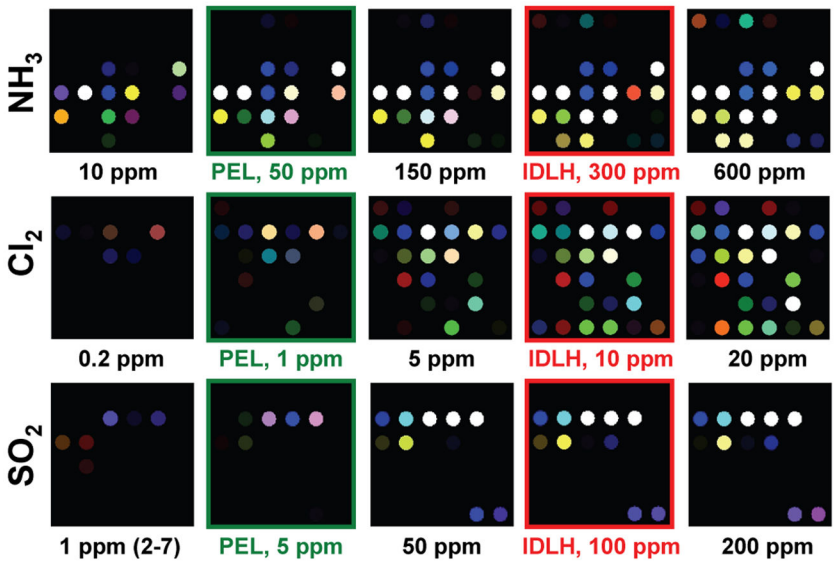

Fig. 3. The effect of concentration on array response to NH_3, Cl_2, and SO_2

The color change profiles of these three representative TICs are shown over roughly a hundred-fold range of concentration. The observed limits of detection (LOD) are well below the PEL (permissible exposure limit). For display purposes, the color range of these difference maps are expanded from 4 to 8 bits per color (RGB range of 4–19 expanded to 0–255), except for SO_2 at 1 ppm (RGB range of 2–7).

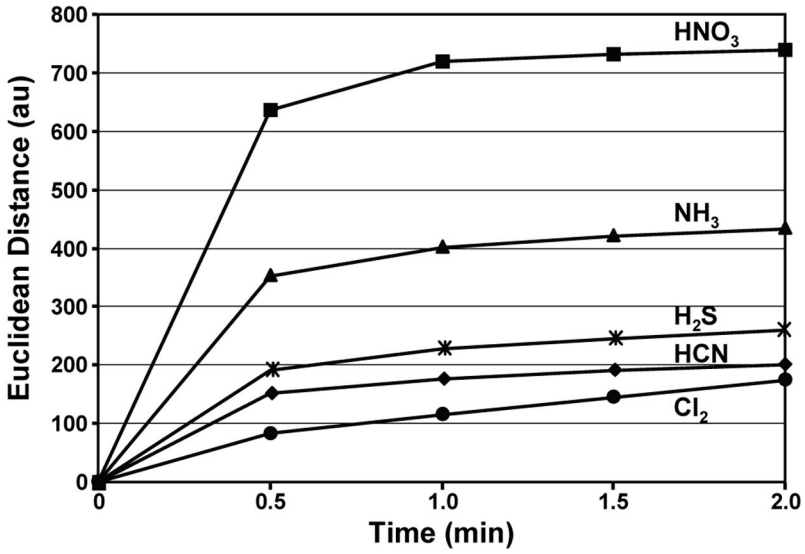

Fig. 4. Response time of the array

Total Euclidean distance of the array is plotted versus time for five representative TICs at their IDLH concentrations; the average of seven trials is shown. The Euclidean distance is simply the total length of the 108-dimensional color difference vector, i.e., the total array response.

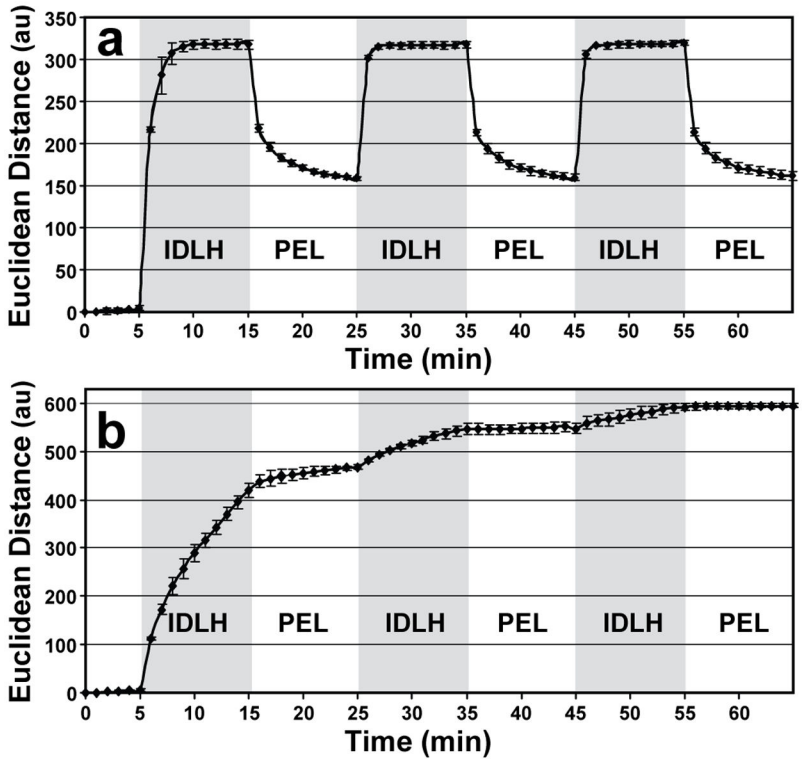

Fig. 5. Reversibility of colorimetric array response

a, SO_2 exposure of the array from N_2 to the IDLH (100 ppm) level, and then repeatedly from the IDLH to PEL (5 ppm) and back. **b**, Cl_2 exposure of the array from N_2 to the IDLH (10 ppm) level, and then repeatedly from the IDLH to PEL (1 ppm) and back. Data was acquired every min. The response times in this data reflect the dead volume in the gas mixing system and do not represent the intrinsic response of the array (which is shown in Fig. 4). The error bars shown are the standard deviation of triplicate trials.

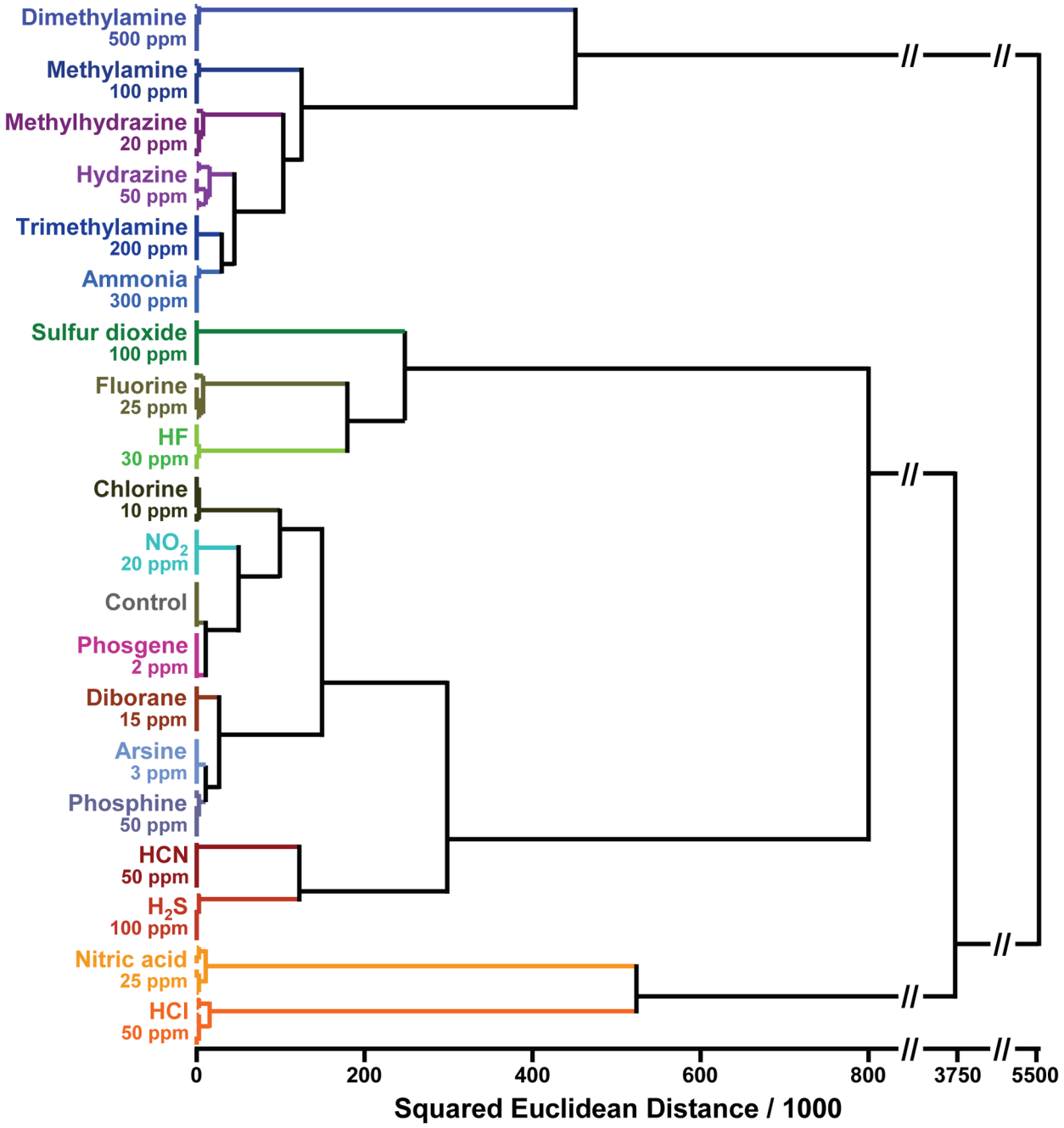

Fig. 6. Hierarchical cluster analysis (HCA) for 19 TICs at IDLH concentrations and a control

HCA is a routine model-free statistical classification method based on Euclidean distance37–40. In these experiments, the Euclidean distances are defined by the color difference vectors of each experimental trial in the full 108-dimensional space made up of the changes in red, green, and blue values of the 36 nanoporous pigments in the sensor array. As shown, all experiments were run in septuplicate: *no confusions or errors in classification were observed in 140 trials*. The IDLH concentrations of each analyte are shown in ppm. The HCA used minimum variance (i.e., “Ward’s Method”) for clustering.